Requirement of Rac1 in the development of cardiac hypertrophy

Minoru Satoh*, Hisakazu Ogita*, Kyosuke Takeshita*, Yasushi Mukai*, David J. Kwiatkowski†, and James K. Liao*‡

*Cardiovascular and †Hematology Divisions, Department of Medicine, Brigham and Women's Hospital, Harvard Medical School, Boston, MA 02115

The development of cardiac hypertrophy is mediated, in part, by increase in NADPH oxidase activity and myocardial oxidative stress. The Rho GTPase, Rac, regulates NADPH oxidase activity through interaction with gp91^{phox} and p67^{phox} (in which "phox" is phagocyte oxidase). However, it is not known which Rac isoform mediates this effect in the heart. Here we show that Rac1 is critical for generating oxidative stress and producing cardiac hypertrophy in the adult heart. The Rac1 gene was temporally and specifically deleted in adult mouse cardiomyocytes (c-Rac1$^{-/-}$). Compared with wild-type or Rac1 heterozygous mice, the hearts of c-Rac1$^{-/-}$ mice showed decreased gp91^{phox} and p67^{phox} interaction, NADPH oxidase activity, and myocardial oxidative stress in response to angiotensin II (400 ng/kg per day for 2 weeks) stimulation. This result correlated with decreased myocardial hypertrophy. These results indicate that Rac1 is critical for the hypertrophic response in the heart and suggest that therapies which target myocardial Rac1 may be beneficial in the treatment of cardiac hypertrophy.

small G protein | oxidative stress | angiotensin II | NADPH oxidase

Cardiac hypertrophy leading to heart failure is a major cause of morbidity and mortality worldwide (1). In response to pressure overload, the myocardium secretes vasoactive substances such as angiotensin II (Ang II), which in turn induce various intracellular signaling pathways that contribute to the hypertrophic response. Recent studies suggest that the hypertrophic response is mediated by increase in intracellular oxidative stress (2, 3). The source of oxidative stress in cardiac hypertrophy is not known, but evidence suggests that in cardiomyocytes, a phagocytic-type NADPH oxidase may be an important source of reactive oxygen species (4–6).

The NADPH oxidase is a multicomponent enzyme complex that consists of the membrane-bound cytochrome b_{558}, which contains gp91^{phox} and p22^{phox} (in which "phox" is phagocyte oxidase), the cytosolic regulatory subunits, p47^{phox} and p67^{phox}, and the small GTP-binding protein Rac (7). In particular, Rac, which mediates the hetero-dimerization of gp91^{phox} with p67^{phox}, is critical for the assembly and function of this multicomponent NADPH oxidase complex (8, 9). Rac has three isoforms, the ubiquitously expressed Rac1, a hematopoietic cell-specific isoform Rac2, and Rac3, a close relative of Rac1, which appears to be expressed in brain, lung, liver, and pancreas (10). Rac1 is reported to be the component of NADPH oxidase in nonphagocytic cells (11). Rac2 is known to be the essential isoform for NADPH oxidase in neutrophils (12). However, it is not known which Rac isoform mediates NADPH oxidase activity in the heart.

There is evidence that Rac1 participates in the myocardial hypertrophic response. Adenoviral-mediated gene transfer of a constitutively active isoform of Rac1 (V12rac1) in neonatal cardiac myocytes results in sarcomeric reorganization and an increase in cell size that is indistinguishable from phenylephrine-stimulated hypertrophy (13). Induction of V12rac1 in mouse heart leads to cardiomyopathic changes characterized by hypertrophy or dilation (14). In contrast, overexpression of a dominant-negative mutant form of Rac1 (N17rac1) suppresses phenylephrine-induced myocardial oxidative stress and hypertrophy

in vitro (13). However, the requirement of Rac1 in mediating the hypertrophic process, especially in the adult heart, has not been demonstrated.

Although previous studies with dominant-negative and gain-of-function models of Rac1 suggest the importance of Rac1 in the development of cardiac hypertrophy, loss of function or gene deletion of Rac1 is generally considered to be more conclusive. Therefore, tissue-specific deletion, which uses the Cre/loxP technology (15), offers the best strategy for studying the adult phenotype of Rac1 deletion. To achieve this deletion, we used mutant mice containing a conditional or "floxed" allele of Rac1 in which the Rac1 gene can be deleted in a selected cell population (12). However, because gene deletion of Rac1 could potentially lead to embryonic lethality, we developed a transgenic mouse harboring a tamoxifen-inducible Cre-fusion protein under the control of the inducible cardiomyocyte-specific α-myosin heavy-chain promoter (αMHC-MerCreMer). Using these αMHC-MerCreMer mice and the conditional Rac1 knockout mice (12) to generate cardiomyocyte-specific Rac1 deletion (c-Rac1$^{-/-}$) mice, we tested the hypothesis that cardiomyocyte-specific Rac1 deletion inhibits myocardial oxidative stress and the development of cardiac hypertrophy in response to Ang II.

Results

Development of Inducible _Rac1_ Gene Deletion in the Heart. The early embryonic lethality observed in Rac1 knockout mice, which was due to developmental defects in the formation of germ layers during gastrulation (16), has precluded investigating the role of Rac1 in adult cardiac hypertrophy. To bypass this early embryonic lethality, we developed mutant mice with conditional Rac1 allele, which could be deleted in cardiomyocytes in a tissue-specific and temporal manner. The tamoxifen-inducible αMHC-MerCreMer mice were developed by using the αMHC-MerCreMer cDNA construct obtained from Michael Reth (University of Freiburg, Freiburg, Germany) injected into C57BL/6 eggs. These mice are similar to the αMHC-MerCreMer mice previously developed by Molkentin and colleagues (17), but, in contrast, they are on a different background and have higher inducible Cre expression (data not shown). To achieve inducible cardiomyocyte-specific deletion, we backcrossed mice containing a null and conditional "floxed" Rac1 allele (mixed background of C57BL/6 and SV/129) (12) for eight generations onto C57BL/6 background before crossing with αMHC-MerCreMer mice (C57BL/6 background) to obtain αMHC-MerCreMer/Rac1$^{flox/-}$ (Rac1$^{flox/-}$) mice (Fig. 1A). All
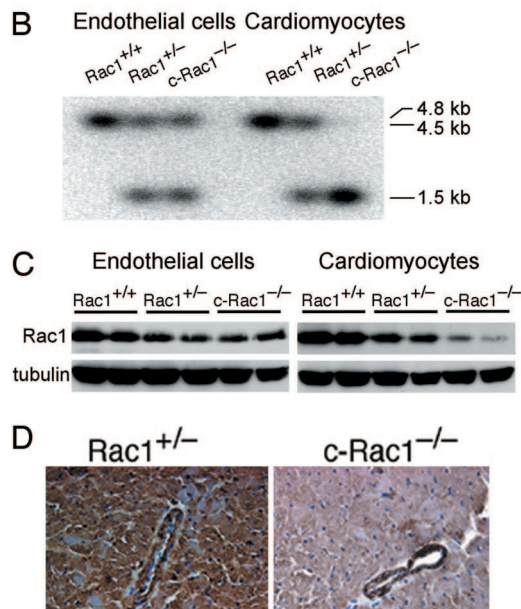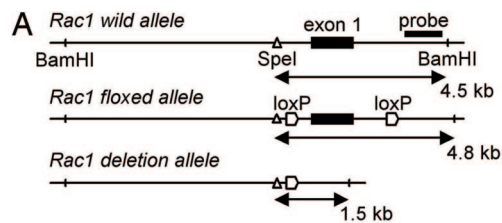

Fig. 1. Generation of inducible cardiomyocyte-specific *Rac1* deletion mice. (*A*) Schematics of the *Rac1* wild, floxed, and deletion alleles. The exon 1 is shown as closed boxes. Horizontal lines with arrows indicate the expected sizes of DNA bands in Southern blotting of the wild, floxed, and deletion alleles. The location of the BamHI and SpeI restriction sites are shown. (*B*) Southern blot analysis of the genomic DNA from isolated ventricular endothelial cells or cardiomyocytes of Rac1$^{+/+}$, Rac1$^{+/-}$, and c-Rac1$^{-/-}$ mice with 4OHT after BamHI and SpeI digestion. (*C*) Immunoblot of Rac1 from the isolated ventricular endothelial cells (*Left*) or cardiomyocytes (*Right*) of Rac1$^{+/+}$, Rac1$^{+/-}$, and c-Rac1$^{-/-}$ mice with 4OHT. (*D*) Representative immunohistochemical staining of Rac1 in the left ventricle from Rac1$^{+/-}$ and c-Rac1$^{-/-}$ mice with 4OHT.

of the mice used in this study including controls were littermates of the same generation.

To produce c-Rac1$^{-/-}$ mice, the Rac1$^{flox/-}$ mice were injected with 2.0 mg of 4-hydroxytamoxifen (4OHT) per day for 5 consecutive days per week for 2 weeks. Because the efficiency of Cre-mediated deletion is somewhat limited (90% for a single allele and 53–65% for cardiomyocytes; data not shown), we generated c-Rac1$^{-/-}$ mice from Rac1$^{flox/-}$ mice rather than from αMHC-MerCreMer/Rac1$^{flox/flox}$ mice. After 4OHT treatment, Cre-mediated excision of *Rac1* allele was observed only in the cardiomyocytes but not in the endothelial cells of c-Rac1$^{-/-}$ mouse heart (Fig. 1*B*). The *Rac1* deletion allele was also not observed in the hearts of 4OHT-treated αMHC-MerCreMer/Rac1 wild-type (Rac1$^{+/+}$) mice. Furthermore, Rac1 expression was comparable in αMHC-MerCreMer/Rac1$^{flox/-}$ mice compared with Rac1$^{flox/-}$ mice, and similar reductions in Rac1 expression in the heart was observed in both mice after 4OHT treatment. In αMHC-MerCreMer/Rac1$^{+/-}$ mice, treatment with 4OHT had no effect on cardiac Rac1 expression compared with that of heterozygous Rac1$^{+/-}$ mice or untreated αMHC-MerCreMer/Rac1$^{+/-}$ mice, indicating that neither the presence of the Cre transgene nor treatment with 4OHT affected Rac1
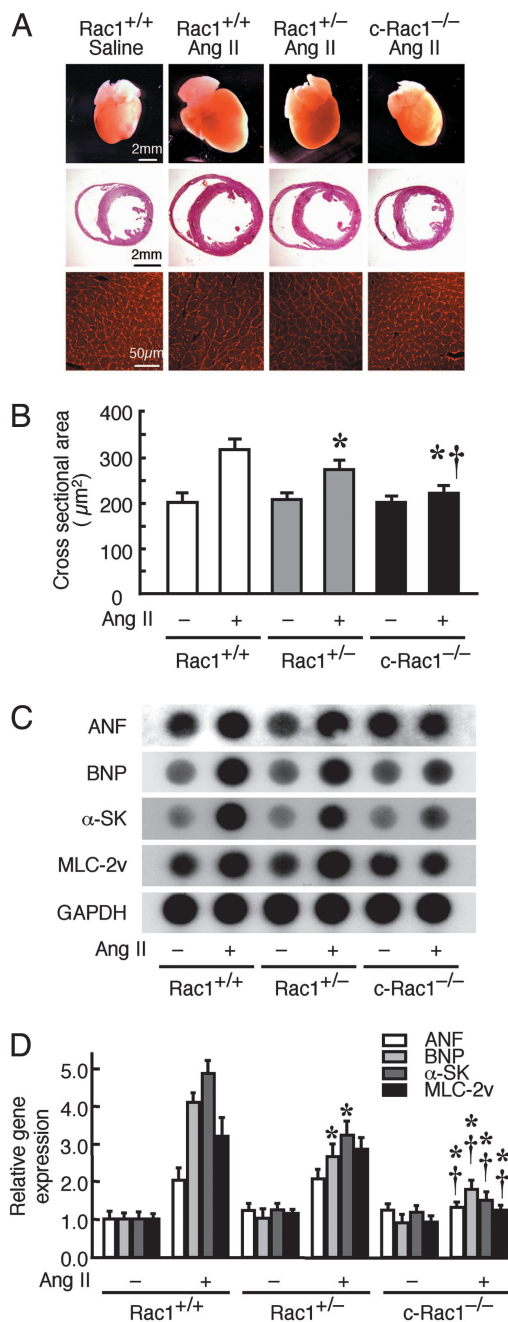

Fig. 2. Decreased cardiac hypertrophy in cardiac-specific *Rac1* deletion mice. (*A*) (*Top*) Representative pictures of hearts from 4OHT-treated Rac1$^{+/+}$, Rac1$^{+/-}$, and c-Rac1$^{-/-}$ mice at 2 weeks after saline or Ang II infusion. (Scale bar: 2 mm.) (*Middle*) Hematoxylin and eosin stain of perfused-fixed heart in cross sections. (Scale bar: 2 mm.) (*Bottom*) Wheat-germ agglutinin stain of myocardial cross sections. (Scale bar: 50 μm.) (*B*) Myocardial cross-sectional area (*n* = 10 in each group). Results are presented as mean ± SD. *, *P* < 0.05 compared with Ang II-treated Rac1$^{+/+}$ mice; †, *P* < 0.05 compared with Ang II-treated Rac1$^{+/-}$ mice. (*C*) RNA dot-blot analysis of cardiac gene fetal expression from Rac1$^{+/+}$, Rac1$^{+/-}$, and c-Rac1$^{-/-}$ mice. ANF, atrial natriuretic factor; BNP, brain natriuretic factor; α-SK, α-skeletal actin; MLC-2v, myosin light chain 2 ventricular isoform. (*D*) Quantitative analysis of mRNA expressions (*n* = 10 in each group). Results are presented as mean ± SD. *, *P* < 0.05 compared with Ang II-treated Rac1$^{+/+}$ mice; †, *P* < 0.05 compared with Ang II-treated Rac1$^{+/-}$ mice.

expression in the absence of *Rac1* floxed allele. Treatment of αMHC-MerCreMer/Rac1$^{flox/-}$ mice with 4OHT (i.e., to generate c-Rac1$^{-/-}$) decreased Rac1 protein expression in cardiomy-
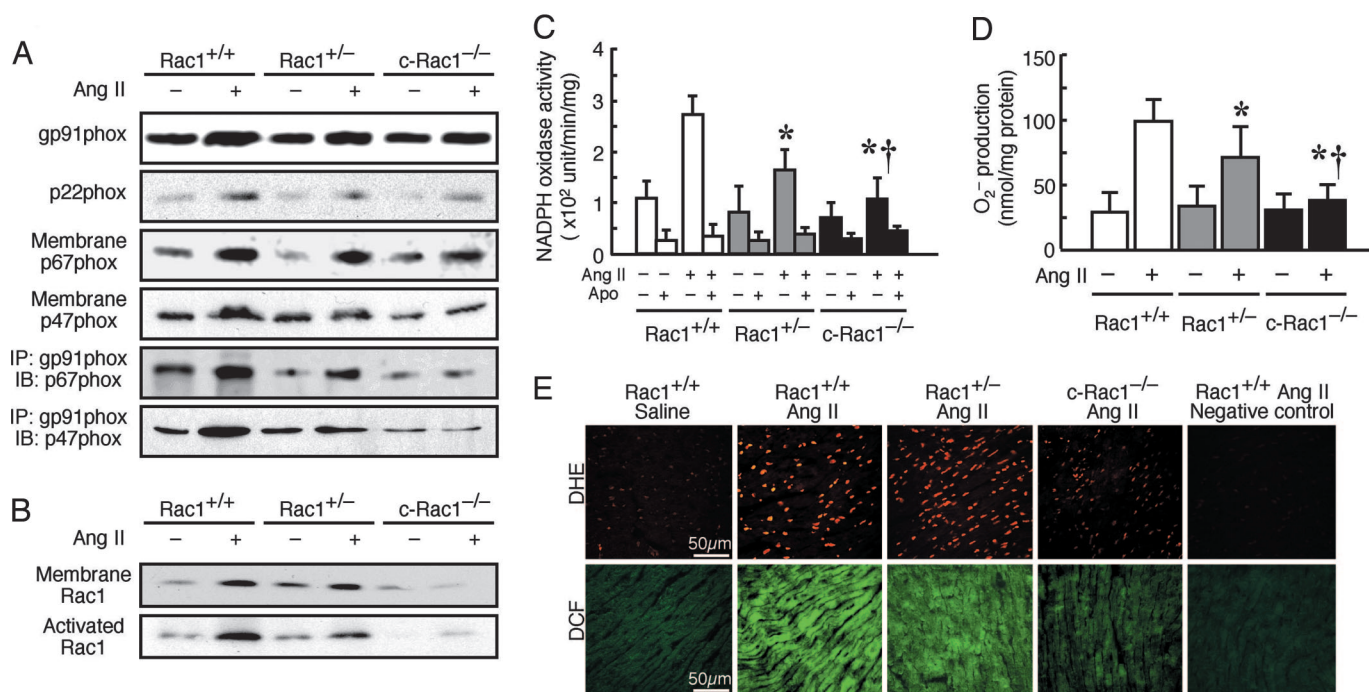
Fig. 3. NADPH oxidase activity and superoxide anion ($O_2^{\bullet-}$) production in cardiac-specific *Rac1* deletion mice. (*A*) Representative immunoblot of NADPH oxidase components gp91^{phox}, p22^{phox}, p67^{phox}, and p47^{phox} in membrane fractions in the hearts of 4OHT-treated Rac1$^{+/+}$, Rac1$^{+/-}$, and c-Rac1$^{-/-}$ mice at 2 weeks after saline or Ang II infusion ($n = 10$ in each group). Membrane fractions in the hearts were also immunoprecipitated (IP) with gp91^{phox} antibody, followed by immunoblotting (IB) with p67^{phox} or p47^{phox} antibody. (*B*) Representative immunoblot of membrane-bound Rac1 and GTP-bound "activated" Rac1 determined by Rac1 pull-down assay. (*C*) NADPH oxidase activity as determined by lucigenin chemiluminescence assay with or without apocynin (Apo) in hearts of Rac1$^{+/+}$, Rac1$^{+/-}$, and c-Rac1$^{-/-}$ mice ($n = 10$ in each group). Results are presented as mean ± SD. *, $P < 0.05$ compared with Ang II-treated Rac1$^{+/+}$ mice; †, $P < 0.05$ compared with Ang II-treated Rac1$^{+/-}$ mice. (*D*) Superoxide anion ($O_2^{\bullet-}$) production as determined by superoxide dismutase-inhibitable ferricytochrome *c* reduction assay in hearts of Rac1$^{+/+}$, Rac1$^{+/-}$, and c-Rac1$^{-/-}$ mice ($n = 10$ in each group). Results are presented as mean ± SD. *, $P < 0.05$ compared with Ang II-treated Rac1$^{+/+}$ mice; †, $P < 0.05$ compared with Ang II-treated Rac1$^{+/-}$ mice. (*E*) Fresh frozen heart tissues from Rac1$^{+/+}$, Rac1$^{+/-}$, and c-Rac1$^{-/-}$ mice with saline or Ang II infusion were stained with dihydroethidium (DHE, red fluorescence) (*Upper*) or 5-(6)-chloromethyl-2',7'-dichlorodihydrofluorescein diacetate (DCF, green fluorescence) (*Lower*). In negative control, heart sections were preincubated with the $O_2^{\bullet-}$ scavenger, tiron. (Scale bar: 50 μm.)

ocytes but not in endothelial cells, whereas Rac1 expression was decreased in both cell types in Rac1$^{+/-}$ mice (Fig. 1*C*). The mRNA expression of Rac1 was also decreased in cardiomyocytes of c-Rac1$^{-/-}$ mice (see Fig. 5*A*, which is published as supporting information on the PNAS web site). Although Rac2 could also participate in NADPH oxidase activity, neither Rac2 nor Rac3 was detected in cardiomyocytes in all groups of mice (Fig. 5*B*). Immunohistochemical staining showed that Rac1 was expressed in cardiomyocytes and endothelial cells in Rac1$^{+/-}$ mice (Fig. 1*D*). In contrast, Rac1 expression was not observed in cardiomyocytes in c-Rac1$^{-/-}$ mice, whereas its expression in the endothelial cells was unchanged compared with that of Rac1$^{+/-}$ mice.

Decreased Cardiac Hypertrophy in Cardiac-Specific *Rac1* Deletion Mice. There were no differences in basal body weight, basal blood pressure, left ventricular (LV) volume, and cardiac function in Rac1$^{+/+}$, Rac1$^{+/-}$, and c-Rac1$^{-/-}$ mice with or without 4OHT. Despite similar increases in systolic blood pressure by Ang II infusion in all three groups (i.e., 15% increase), Rac1$^{+/-}$ mice and, to a lesser extent, c-Rac1$^{-/-}$ mice, showed decreased cardiac hypertrophy (Fig. 2*A*), reduced end-diastolic myocardial wall thickness (intraventricular septum, posterior wall) and LV mass (Table 1, which is published as supporting information on the PNAS web site), and smaller induction of cardiac fetal gene expression (ANF, atrial natriuretic factor; BNP, brain natriuretic peptide; α-SK, α-skeletal actin; and MLC-2v, myosin light chain-2 ventricular isoform) (Fig. 2 *C* and *D*) and heart weight-to-tibial length ratio compared with that of Rac1$^{+/+}$ mice (Table 1).

Echocardiographic study showed that, compared with saline infusion, Ang II increased LV mass by 184, 160, and 123% in Rac1$^{+/+}$, Rac1$^{+/-}$, and c-Rac1$^{-/-}$ mice, respectively. Similar to the echocardiographic findings, cardiomyocyte cross-sectional areas were also increased in the Rac1$^{+/+}$ mice in response to Ang II (330 ± 20 vs. 200 ± 20 μm^2; $P < 0.01$ compared with baseline) (Fig. 2*B*). Smaller increases in cross-sectional area were observed in the hearts of Rac1$^{+/-}$ mice (270 ± 20 μm^2; $P < 0.05$ vs. Rac1$^{+/+}$ mice), whereas hearts from c-Rac1$^{-/-}$ mice showed no increase in cross-sectional area in response to Ang II (220 ± 20 μm^2; $P < 0.05$ vs. Rac1$^{+/-}$ mice). These results indicate that myocardial Rac1 is critical for the development of cardiac hypertrophy.

Decreased NADPH Oxidase Activity in Cardiac-Specific *Rac1* Deletion Mice. Because Rac1 plays an important role in the assembly and function of membrane-bound NADPH oxidase, we assessed NADPH oxidase expression and activity in the hearts of c-Rac1$^{-/-}$ mice. Treatment with Ang II increased the expression of membrane components, gp91^{phox} and p22^{phox}, to a similar extent in Rac1$^{+/+}$, Rac1$^{+/-}$, and c-Rac1$^{-/-}$ mice. However, the association of p47^{phox} and p67^{phox} with the membrane was not increased by Ang II in the c-Rac1$^{-/-}$ mice compared with that of Rac1$^{+/+}$ and Rac1$^{+/-}$ mice (Fig. 3*A*). The interaction of gp91^{phox} with p67^{phox} was increased by Ang II in Rac1$^{+/+}$ mice, increased to a lesser extent in Rac1$^{+/-}$ mice, and not affected in c-Rac1$^{-/-}$ mice. The interaction of gp91^{phox} with p47^{phox} was also attenuated in c-Rac1$^{-/-}$ mice. This finding corresponded to decreased membrane-bound Rac1 and Rac1 activation in the

hearts of c-Rac1$^{-/-}$ mice (Fig. 3B). Treatment with Ang II increased NADPH oxidase activity to a greater extent in the hearts of Rac1$^{+/+}$ mice compared with that of Rac1$^{+/-}$ mice (280 ± 50 vs. 170 ± 50 units/min per mg; $P < 0.05$) (Fig. 3C). Compared with Rac1$^{+/-}$ mice, the Ang II-induced NADPH oxidase activity was lower in the hearts of c-Rac1$^{-/-}$ mice (110 ± 40 units/min per mg; $P < 0.05$). However, in the kidneys, the Ang II-induced NADPH oxidase activities were similar in Rac1$^{+/-}$ and c-Rac1$^{-/-}$ mice ($3,610 \pm 980$ vs. $3,860 \pm 860$ units/min per mg; $P > 0.05$), and both levels were substantially lower compared with the NADPH activity in the kidney of Rac1$^{+/+}$ mice ($4,780 \pm 1,270$ units/min per mg; $P < 0.05$ vs. Rac1$^{+/-}$ or c-Rac1$^{-/-}$ mice) (see Fig. 6A, which is published as supporting information on the PNAS web site).

Decreased Superoxide Anion Production in Cardiac-Specific *Rac1* Deletion Mice. To determine whether NADPH oxidase is the primary source of intracellular myocardial oxidative stress in response to Ang II, we measured $O_2^{\cdot-}$ production in c-Rac1$^{-/-}$ mice. Using ferricytochrome c reduction assay, we found that basal $O_2^{\cdot-}$ production as determined in the presence of apocynin was comparable in all of the mice. Treatment with Ang II increased $O_2^{\cdot-}$ production by 3.3-fold in heart tissues from Rac1$^{+/+}$ mice (Fig. 3D). However, in Rac1$^{+/-}$ and c-Rac1$^{-/-}$ mice, $O_2^{\cdot-}$ production was increased by only 2.1- and 1.2-fold, respectively ($P < 0.05$ compared with Rac1$^{+/+}$ for both, and $P < 0.05$ compared with each other). Similar to NADPH oxidase activity, the increase in $O_2^{\cdot-}$ production was comparably lower in the kidney of Rac1$^{+/-}$ and c-Rac1$^{-/-}$ mice (1.4-fold vs. 1.5-fold, $P > 0.05$) compared with that of Rac1$^{+/+}$ mice (1.9-fold, $P < 0.05$) (Fig. 6B). The effects of *Rac1* deletion on Ang II-induced $O_2^{\cdot-}$ production corresponded to changes in intracellular myocardial oxidative stress. The increase in reactive oxygen species generation and peroxide-derived oxygen radicals as qualitatively determined by staining with dihydroethidium and dichlorofluorescein, respectively, in fresh frozen heart sections, were increased in Rac1$^{+/+}$ mice and substantially attenuated in c-Rac1$^{-/-}$ mice (Fig. 3E). These findings indicate that the predominant source of $O_2^{\cdot-}$ production in the heart in response to Ang II is the Rac1-dependent NADPH oxidase.

Decreased Ang II-Induced Apoptosis Signal-Regulating Kinase 1 (ASK1) and NF-κB Activity in Cardiac-Specific *Rac1* Deletion Mice. To assess potential downstream targets of reactive oxygen species signaling which could affect the hypertrophic response, we investigated the activities of the redox-sensitive mitogen-activated protein kinase kinase, ASK1, and transcription factor NF-κB in wild-type and *Rac1* mutant mice. The activation of ASK1 or NF-κB mediates cardiac myocyte hypertrophy *in vitro* (18). Treatment with Ang II increased ASK1 activity in Rac1$^{+/+}$ mice. Ang II-induced ASK1 activity was decreased in Rac1$^{+/-}$ mice and completely inhibited in c-Rac1$^{-/-}$ mice (Fig. 4 A and B). Similarly, the activation of NF-κB in response to Ang II was observed in the hearts of Rac1$^{+/+}$ mice, was observed to a lesser extent in the hearts of Rac1$^{+/-}$ mice, and was not observed at all in the hearts of c-Rac1$^{-/-}$ mice (Fig. 4 C and D). These findings indicate that the activation of ASK1 and NF-κB depends on Rac1 and suggest that ASK1 and NF-κB may participate in some of the downstream effects of Rac1 and NADPH oxidase on cardiac hypertrophy.

Discussion

The purpose of this study was to develop the cardiomyocyte-specific *Rac1* deletion mice and to determine whether cardiomyocyte-specific *Rac1* deletion inhibits myocardial oxidative stress and the development of cardiac hypertrophy in response to Ang II. Our findings indicate that Rac1, through interaction with gp91^{phox} and the cytosolic components of NADPH oxidase,
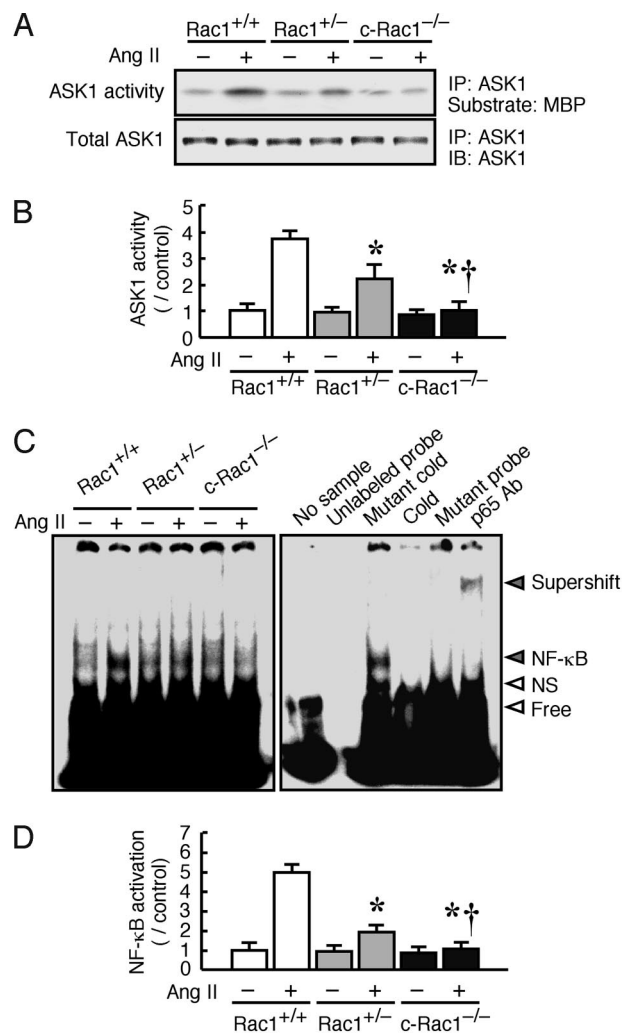

Fig. 4. ASK1 activity and NF-κB activation in cardiac-specific *Rac1* deletion mice. (*A*) (*Upper*) Representative ASK1 activity assay in 4OHT-treated Rac1$^{+/+}$, Rac1$^{+/-}$, and c-Rac1$^{-/-}$ mice heart at 2 weeks after saline or Ang II infusion. Immune complex kinase assays were performed employing myelin basic protein (MBP) in the presence of [γ-^{32}P]ATP. After electrophoresis, the gel was dried and autoradiographed, and the relative intensity of autoradiograms was determined by scanning densitometry. (*Lower*) Heart tissues were also immunoprecipitated (IP) with ASK1 antibody, followed by immunoblotting (IB) with ASK1 antibody. (*B*) Quantification of ASK1 activity ($n = 10$ in each group). Results are presented as mean $\pm$ SD. *, $P < 0.05$ compared with Ang II-treated Rac1$^{+/+}$ mice. †, $P < 0.05$ compared with Ang II-treated Rac1$^{+/-}$ mice. (*C*) (*Left*) Representative electrophoretic mobility shift assay of NF-κB in Rac1$^{+/+}$, Rac1$^{+/-}$, and c-Rac1$^{-/-}$ heart. (*Right*) Specificity of NF-κB binding activity was analyzed by the addition of unlabeled probe or mutant probe, by the pretreatment with excess unlabeled probe (Cold) or mutant probe (Mutant cold), and by anti-p65 antibody (p65 Ab) supershift gel assay. NF-κB binding band (NF-κB), nonspecific binding band (NS), free probe (Free), and the raised bands supershifted by antibody (Supershift) are indicated on the right. (*D*) Quantification of NF-κB activation ($n = 10$ in each group). Results are presented as mean $\pm$ SD. *, $P < 0.05$ compared with Ang II-treated Rac1$^{+/+}$ mice; †, $P < 0.05$ compared with Ang II-treated Rac1$^{+/-}$ mice.

p67^{phox} and p47^{phox}, plays a critical role in the development of cardiac hypertrophy in response to Ang II. Treatment with Ang II activates NADPH oxidase, increases $O_2^{\cdot-}$ production, induces cardiac fetal gene expression, and leads to increased LV mass. All of these effects of Ang II on the heart occurred with similar changes in blood pressure and were decreased or absent in mutant mice with decreased cardiac expression of Rac1. These findings indicate that cardiomyocyte Rac1 plays a pivotal role in

MEDICAL SCIENCES

the development of cardiac hypertrophy in response to Ang II. Clinically, inhibition of Rac1-mediated oxidative stress could be an underlying non-cholesterol-dependent mechanism of 3-hydroxy-3-methylglutaryl CoA reductase inhibitors or statins, which prevent the development of cardiac hypertrophy, through inhibition of protein isoprenylation (2, 19).

An important step in NADPH oxidase assembly is the interaction between p67[phox], active GTP-bound Rac1, and gp91[phox] (4, 8, 9). Studies with Rac1-p67[phox] chimeras, which are covalently linked but contain mutations that prevent a functional Rac1-p67[phox] interaction, support the notion that Rac1 is required to anchor cytosolic p67[phox] to the membrane and to promote an "active form" of p67[phox] (20). Thus, deletion or inhibition of Rac1 leads to diminished Rac1-p67[phox] complex formation and results in diminished activation of NADPH oxidase. Indeed, Ang II-induced $O_2^{\cdot-}$ production is inhibited by a dominant-negative mutant of Rac1 (2). Although Rac2 has been shown to be involved in NADPH oxidase-dependent superoxide anion production (12), we could not detect appreciable levels of Rac2 or Rac3 in the hearts of wild-type or mutant *Rac1* mice, indicating that Rac1 is the predominant Rac isoform that mediates NADPH oxidase activity in cardiomyocytes.

Because Rac1 also regulates actin cytoskeletal assembly and sarcomeric reorganization, it is possible that the decrease in Ang II-induced cardiac hypertrophy may not be entirely due to the inhibition of NADPH oxidase activity and myocardial oxidative stress. Indeed, overexpression of constitutively active Rac1 induces phenotypic changes in cardiomyocytes characterized by increase in cell size that is indistinguishable from phenylephrine-induced hypertrophy (13, 14). Whether these changes are merely associated with, rather than mediated by, increase in NADPH oxidase activity remains to be determined. For example, it is possible that deletion of *Rac1* gene could also interfere with the expression of proteins that are involved in Ang II signaling, such as angiotensin AT1 receptor. Although we did not find any changes in AT1 receptor expression in the cardiomyocytes of Rac1^{+/+}, Rac1^{+/−}, and c-Rac1^{−/−} mice (see Fig. 7, which is published as supporting information on the PNAS web site), this result does not exclude the possibility that *Rac1* deletion could affect other downstream targets of Ang II signaling. Nevertheless, in support of a causative effect of NADPH oxidase on cardiac hypertrophy are previous studies showing that mice with targeted disruption of gp91[phox] have decreased myocardial superoxide anion production and developed less cardiac hypertrophy in response to Ang II (5). Our results are in agreement with these studies and support the notion that Rac1-mediated NADPH oxidase activity and not some other effects of Rac1 is the primary regulator of cardiac hypertrophy in response to Ang II.

In summary, we have shown that cardiomyocyte-specific *Rac1* deletion prevents Ang II-induced cardiac hypertrophy. Rac1 is a critical component for NADPH oxidase and is required for Ang II-induced superoxide anion production in cardiomyocytes. These findings suggest that therapies, which target myocardial Rac1, may be beneficial for the treatment of cardiac hypertrophy. It remains to be determined how increase in oxidative stress can activate the diverse intracellular signaling pathways that lead to the development of cardiac hypertrophy, and more importantly, to the transition between compensated cardiac hypertrophy and heart failure.

Materials and Methods

Generation of Inducible Cardiomyocyte-Specific *Rac1* Deletion in Mice.
Rac1 conditional floxed mice (mixed background of C57BL/6 and SV/129) were generated as described in ref. 12 and were backcrossed eight times onto the C57/BL6 strain. The αMHC-MerCreMer transgenic mice (C57BL/6 background) were developed at the Brigham and Women's Hospital using the

αMHC-MerCreMer cDNA construct from Michael Reth. These mice are similar to the αMHC-MerCreMer mice reported in ref. 17, except that these mice are on C57BL/6 background and exhibit higher inducibility of Cre-mediated excision with tamoxifen. To obtain a cardiomyocyte-specific inducible deletion of the *Rac1* gene, we bred mice that have homozygous *Rac1* conditional floxed allele or were heterozygous to the *Rac1* wild-type allele with αMHC-MerCreMer mice, which resulted in the generation of mice with genotypes of αMHC-MerCreMer/Rac1[flox/+] or Rac1^{+/−}. Next, these mice were mated with each other, and we obtained the mice with genotypes of αMHC-MerCreMer-positive Rac1^{+/+}, Rac1^{+/−}, and Rac1[flox/−]. These mice grow normally into adulthood without any health problems. To obtain the c-Rac1^{−/−} mice, 2.0 mg of 4OHT was injected intraperitoneally into 6- to 8-week-old Rac1[flox/−] mice for 5 consecutive days per week for 2 weeks. All mice, including littermate male Rac1^{+/+} and Rac1^{+/−} mice, received 4OHT injection to exclude potential confounding effects of 4OHT treatment. All experimental procedures on animals were performed by using protocols accepted by the Harvard Medical School's Standing Committee on Animal Welfare and Protection and are in accordance with the *Guide for the Care and Use of Laboratory Animals*, published by the National Institutes of Health.

Isolation of Cardiomyocytes and Endothelial Cells from the Heart.
Cardiomyocytes were isolated from ventricles of Rac1^{+/+}, Rac1^{+/−}, or c-Rac1^{−/−} mice as described in refs. 2 and 6. Heart endothelial cells were isolated by two-step immunoselection with platelet endothelial cell adhesion molecule-1- and intercellular adhesion molecule-2-conjugated magnetic beads as described in refs. 21 and 22.

Southern Blotting.
Genomic DNA isolated from mouse cardiomyocytes or heart endothelial cells was digested with BamHI and SpeI and hybridized with the 3′ probe. Further details are provided in *Supporting Materials and Methods*, which is published as supporting information on the PNAS web site.

Ang II Infusion.
One week after the last injection of 4OHT, the pumps were implanted into male mice (11–13 weeks old) s.c. Ang II (400 ng/kg per min) dissolved in saline or saline was infused with microosmotic pumps (model 2004; Durect, Cupertino, CA) for 2 weeks as described (23). The treatment groups contained at least 12 mice in each group (i.e., Rac1^{+/+}, Rac1^{+/−}, and c-Rac1^{−/−} mice).

Blood Pressure and Echocardiographic Measurement.
Both noninvasive systolic blood pressure and heart rate were measured by the tail-cuff method in nonsedated, awake mice. Transthoracic echocardiography was performed with 15-MHz pulse-wave Doppler echocardiography (SONOS 4500; Hewlett–Packard) as described (23). All recordings were performed on conscious animals.

Histological Analysis.
Heart tissue was embedded in Tissue-Tek OCT compound (Electron Microscopy Sciences, Hatfield, PA) and snap-frozen in acetone chilled in dry ice. Unfixed 6-μm cryosections were stained with Texas red-X-conjugated wheat germ agglutinin (Molecular Probes) to evaluate myofiber size. Average data reflect results from 5–6 hearts in each group (8–10 regions per heart). Some hearts were fixed with 4% paraformaldehyde perfusion, and 6-μm cryosections were stained with hematoxylin and eosin.

Immunohistochemistry.
Cryosections (6 μm) fixed in 4% buffered paraformaldehyde were stained with an antibody against Rac1

(Santa Cruz Biotechnology). Detection was carried out by using the EnVision+ system and diaminobenzidine (DAKO).

RT-PCR. Total mRNA was extracted from isolated cardiomyocytes with TRIzol reagents (Invitrogen) according to the manufacturer's protocol. RT-PCR assays were performed as described (24). PCR products were separated on 0.8% agarose gel and stained with ethidium bromide. Further details are provided in *Supporting Materials and Methods*.

RNA Dot-Blot Analysis. Total mRNA (2 μg) was used in dot-blot analysis following an established protocol with previously published oligonucleotide probes for atrial natriuretic factor, brain natriuretic factor, α-skeletal actin, myosin light chain 2 ventricular isoform, and GAPDH (25). The mean relative steady-state transcript levels were calculated and expressed as a percentage of the saline-treated Rac1$^{+/+}$ mice levels after normalization to the GAPDH signal.

Protein Preparation and Immunoblotting. Membrane proteins or total heart, kidney, cardiomyocyte, and heart endothelial cell lysates were extracted as described (26). Protein samples (50 μg per lane) were subjected to immunoblotting analysis using antibodies against gp91^{phox}, p67^{phox}, p47^{phox}, and Rac1 from Upstate Biotechnology (Lake Placid, NY), and antibodies against p22^{phox} and tubulin from Santa Cruz Biotechnology. For detection of NADPH oxidase complex, we performed immunoprecipitation with anti-gp91^{phox} antibody followed by immunoblotting with anti-p67^{phox} or p47^{phox} antibody. For detection of ASK1, we performed immunoprecipitation with anti-ASK1 antibody (Santa Cruz Biotechnology) followed by immunoblotting with ASK1. Signals were detected by using the enhanced chemiluminescence system (Amersham Pharmacia Biosciences).

Measurements of Rac1 Activation. Activated Rac1 was determined by p21-binding domain of p21-activated protein kinase 1 pull-down assay (Rac Activation Assay Kit; Upstate Biotechnology) according to the manufacturer's protocol.

Measurements of NADPH Oxidase Activation. NADPH oxidase activity in homogenates of LV and renal cortex was measured by using lucigenin chemiluminescence (6) after addition of NADPH in the absence or presence of apocynin. Further details are provided in *Supporting Materials and Methods*.

Measurement of O$_2^{\bullet-}$ Production. The production of O$_2^{\bullet-}$ in the LV and renal cortex was measured by superoxide dismutase-inhibitable reduction of ferricytochrome *c* as described (27). Rates of O$_2^{\bullet-}$ production were calculated as described (28). In addition, to evaluate the production of tissue reactive oxygen species, fresh frozen left ventricular myocardium (10-μm slices) was incubated for 1 h at 37°C with dihydroethidium (2 μM; Molecular Probes) and 5-(6)-chloromethyl-2′,7′-dichlorodihydrofluorescein diacetate (4 μM; Molecular Probes) as described (2, 6). Negative control sections were preincubated with tiron (O$_2^{\bullet-}$ scavenger, 10 mM).

ASK1 Immune Complex Kinase Assay. The activity of ASK1 was measured by an immune complex kinase assay as described in *Supporting Materials and Methods*.

EMSA. Nuclear proteins were isolated from heart samples and NF-κB activity was examined by EMSA as described (24). A 20-μl binding reaction mixture containing 20 μg of nuclear proteins was incubated with double-stranded NF-κB consensus oligonucleotide labeled with 35 fmols of [γ-^{32}P]ATP. A supershift assay using antibodies to p65 was performed to confirm NF-κB binding specificity as described (24).

Statistics. Values are shown as mean $\pm$ SD. All parameters were evaluated with the Mann–Whitney U test or Kruskal–Wallis test when multiple mean comparisons were required. A P value of <0.05 was considered statistically significant.

1. Levy, D., Garrison, R. J., Savage, D. D., Kannel, W. B. & Castelli, W. P. (1990) *N. Engl. J. Med.* **322,** 1561–1566.
2. Takemoto, M., Node, K., Nakagami, H., Liao, Y., Grimm, M., Takemoto, Y., Kitakaze, M. & Liao, J. K. (2001) *J. Clin. Invest.* **108,** 1429–1437.
3. Sawyer, D. B., Siwik, D. A., Xiao, L., Pimentel, D. R., Singh, K. & Colucci, W. S. (2002) *J. Mol. Cell. Cardiol.* **34,** 379–388.
4. Abo, A., Pick, E., Hall, A., Totty, N., Teahan, C. G. & Segal, A. W. (1991) *Nature* **353,** 668–670.
5. Bendall, J. K., Cave, A. C., Heymes, C., Gall, N. & Shah, A. M. (2002) *Circulation* **105,** 293–296.
6. Nakagami, H., Takemoto, M. & Liao, J. K. (2003) *J. Mol. Cell. Cardiol.* **35,** 851–859.
7. Babior, B. M. (1999) *Blood* **93,** 1464–1476.
8. Diekmann, D., Abo, A., Johnston, C., Segal, A. W. & Hall, A. (1994) *Science* **265,** 531–533.
9. Leusen, J. H., de Klein, A., Hilarius, P. M., Ahlin, A., Palmblad, J., Smith, C. I., Diekmann, D., Hall, A., Verhoeven, A. J. & Roos, D. (1996) *J. Exp. Med.* **184,** 1243–1249.
10. Haataja, L., Groffen, J. & Heisterkamp, N. (1997) *J. Biol. Chem.* **272,** 20384–20388.
11. Zuo, L., Ushio-Fukai, M., Ikeda, S., Hilenski, L., Patrushev, N. & Alexander, R. W. (2005) *Arterioscler. Thromb. Vasc. Biol.* **25,** 1824–1830.
12. Glogauer, M., Marchal, C. C., Zhu, F., Worku, A., Clausen, B. E., Foerster, I., Marks, P., Downey, G. P., Dinauer, M. & Kwiatkowski, D. J. (2003) *J. Immunol.* **170,** 5652–5657.
13. Pracyk, J. B., Tanaka, K., Hegland, D. D., Kim, K. S., Sethi, R., Rovira, II, Blazina, D. R., Lee, L., Bruder, J. T., Kovesdi, I., *et al.* (1998) *J. Clin. Invest.* **102,** 929–937.
14. Sussman, M. A., Welch, S., Walker, A., Klevitsky, R., Hewett, T. E., Price, R. L., Schaefer, E. & Yager, K. (2000) *J. Clin. Invest.* **105,** 875–886.
15. Gu, H., Marth, J. D., Orban, P. C., Mossmann, H. & Rajewsky, K. (1994) *Science* **265,** 103–106.
16. Sugihara, K., Nakatsuji, N., Nakamura, K., Nakao, K., Hashimoto, R., Otani, H., Sakagami, H., Kondo, H., Nozawa, S., Aiba, A. & Katsuki, M. (1998) *Oncogene* **17,** 3427–3433.
17. Sohal, D. S., Nghiem, M., Crackower, M. A., Witt, S. A., Kimball, T. R., Tymitz, K. M., Penninger, J. M. & Molkentin, J. D. (2001) *Circ. Res.* **89,** 20–25.
18. Higuchi, Y., Otsu, K., Nishida, K., Hirotani, S., Nakayama, H., Yamaguchi, O., Hikoso, S., Kashiwase, K., Takeda, T., Watanabe, T., *et al.* (2003) *J. Biol. Chem.* **278,** 20770–20777.
19. Nishikawa, H., Miura, S., Zhang, B., Shimomura, H., Arai, H., Tsuchiya, Y., Matsuo, K. & Saku, K. (2004) *Circ. J.* **68,** 121–125.
20. Sarfstein, R., Gorzalczany, Y., Mizrahi, A., Berdichevsky, Y., Molshanski-Mor, S., Weinbaum, C., Hirshberg, M., Dagher, M. C. & Pick, E. (2004) *J. Biol. Chem.* **279,** 16007–16016.
21. Mukai, Y., Rikitake, Y., Shiojima, I., Wolfrum, S., Satoh, M., Takeshita, K., Hiroi, Y., Salomone, S., Kim, H. H., Benjamin, L. E., *et al.* (2006) *J. Clin. Invest.* **116,** 334–343.
22. Lim, Y. C., Garcia-Cardena, G., Allport, J. R., Zervoglos, M., Connolly, A. J., Gimbrone, M. A., Jr., & Luscinskas, F. W. (2003) *Am. J. Pathol.* **162,** 1591–1601.
23. Rikitake, Y., Oyama, N., Wang, C. Y., Noma, K., Satoh, M., Kim, H. H. & Liao, J. K. (2005) *Circulation* **112,** 2959–2965.
24. Satoh, M., Kashihara, N., Yamasaki, Y., Maruyama, K., Okamoto, K., Maeshima, Y., Sugiyama, H., Sugaya, T., Murakami, K. & Makino, H. (2001) *J. Am. Soc. Nephrol.* **12,** 317–325.
25. Jones, G. E., Allen, W. E. & Ridley, A. J. (1998) *Cell Adhes. Commun.* **6,** 237–245.
26. Laufs, U., Kilter, H., Konkol, C., Wassmann, S., Bohm, M. & Nickenig, G. (2002) *Cardiovasc. Res.* **53,** 911–920.
27. Matsubara, T. & Ziff, M. (1986) *J. Immunol.* **137,** 3295–3298.
28. Ohara, Y., Peterson, T. E. & Harrison, D. G. (1993) *J. Clin. Invest.* **91,** 2546–2551.

MEDICAL SCIENCES